HEAT TRANSFER STUDIES FOR SUPERCRITICAL FLUIDS UNDER NATURAL CIRCULATION CONDITIONS

Manish Sharma[1], D.S. Pilkhwal[1], P.K. Vijayan[1] and D. Saha[1]
[1] Reactor Engineering Division, Bhabha Atomic Research Centre
Trombay, Mumbai 400 085 INDIA

Abstract

A test facility has been set up to generate data on heat transfer and pressure drop for supercritical fluids under natural circulation conditions. The experiments have been conducted in the test loop with supercritical carbon-dioxide as well as supercritical water as operating fluids. The heat transfer data generated in the test facility has been compared with various heat transfer correlations available in literature for supercritical fluids. The present paper describes the experimental results and comparisons in detail.

1. Introduction

Supercritical water is being considered as a coolant in some advanced nuclear reactor designs i.e. Supercritical Water Cooled Reactors (SCWRs) on account of its potential to offer high thermal efficiency, compact size, elimination of steam generator, separator & dryer, making it economically competitive. Several SCWR designs with forced circulation of primary coolant have been proposed in the past [1-5]. Supercritical water natural circulation loops are capable of generating density gradients comparable to two-phase natural circulation loops. Hence, natural circulation is also considered as a viable option of heat removal in supercritical water cooled reactors [6-7]. Safety is a key issue in the design of advanced reactors and considerable emphasis is placed on passive safety. Cooling a reactor at full power with natural instead of forced circulation is generally considered as enhancement of passive safety. Natural circulation can also be used for passive decay heat removal after reactor shutdown. Hence, the behaviour of steady state natural circulation with supercritical fluids is of interest for a number of new reactor systems. More over heat transfer characteristics of supercritical fluids under natural circulation conditions is also important. Since supercritical water (SCW) or any other supercritical fluid experiences drastic change in its thermodynamic and transport properties near the pseudo-critical temperature, the heat transfer behavior is quite different form sub-critical convective heat transfer. Dramatic reduction in density near the pseudo-critical temperature results in strong buoyancy and acceleration effects across the cross-section causing unusual flow and heat transfer behaviour. Hence normal heat transfer correlations developed for turbulent flow of conventional fluids with small or moderate property variations like Dittus- Boelter correlation may not be applicable at supercritical conditions.

Several researchers in the past have carried out experimental investigation in to forced convective heat transfer for SCW [8-9] as well as supercritical carbon-dioxide [10-11]. Exhaustive literature search carried out for supercritical water and supercritical carbon-dioxide [12-13] confirmed three heat transfer modes in supercritical pressure fluids: (1) so-called normal heat transfer, (2) improved heat transfer, characterized by higher-than-expected heat transfer coefficient (HTC) values than in the normal heat transfer regime and (3) deteriorated heat transfer, characterized by lower-than-expected HTC values than in the normal heat transfer regime. The expected HTC in the normal heat transfer regime is that calculated by Dittus-Boelter correlation. Improved heat transfer is observed at low heat fluxes and deteriorated heat transfer is observed at higher heat fluxes and lower mass fluxes. In

literature, there is still no unique definition for the onset of heat transfer deterioration because reduction in heat transfer coefficient is gradual as compared to sharp increase in wall temperature (or sharp reduction in heat transfer coefficient) associated with boiling crisis at sub-critical pressure conditions.

Carbon-dioxide can be considered as a good simulant fluid for water at supercritical conditions because of analogous change of properties across the pseudocritical point. The dimensionless correlations for heat transfer coefficient are same for supercritical water and supercritical carbon-dioxide [14-15]. Most studies available in literature have reported forced convective heat transfer in supercritical fluids, whereas studies on natural convective heat transfer are considerably less. Hence it is worth while to investigate heat transfer with supercritical fluids under natural circulation conditions. A test facility has been set up to generate data on heat transfer and pressure drop for supercritical fluids under natural circulation conditions.

2. The Experimental Loop

Figure 1 shows the schematic of the experimental loop. It is a uniform diameter rectangular loop made of 13.88 mm inside diameter stainless steel (SS-347) with outside diameter of 21.34 mm. The loop has two heater test sections and two cooler test sections so that the loop can be operated in any one of the four orientations such as Horizontal Heater Horizontal Cooler (HHHC), Horizontal Heater Vertical Cooler (HHVC), Vertical Heater Horizontal Cooler (VHHC) and Vertical Heater Vertical Cooler (VHVC). The heater was made by uniformly winding nichrome wire over a layer of fiber glass insulation. The cooler was tube-in-tube type with chilled water as the secondary coolant flowing in the annulus. The outer tube forming the annulus had 77.9 mm inside diameter and 88.9 mm outside diameter. The loop had a pressuriser connected at the bottom which takes care of the thermal expansion besides accommodating the cover gas helium above the carbon dioxide. The safety devices of the loop (i.e. rupture disc and relief valve) were installed on top of the pressuriser. The entire loop was insulated with three inches of ceramic mat ($k=0.06$ W/m^2).

2.1 Instrumentation

The loop was instrumented with 44 calibrated K-type thermocouples to measure the primary fluid, secondary fluid and heater outside wall temperatures. Primary fluid temperatures at each location was measured as the average value indicated by two thermocouples inserted diametrically opposite at r/2 from the inside wall whereas secondary fluid temperatures were measured by a single thermocouple located at the tube centre. This was adequate to obtain the average temperature as the temperature fluctuation in the secondary fluid was negligible. The thermocouples used to measure the outside wall temperature were installed flush with the outside surface. To enable this, a longitudinal slot of width equal to the diameter of the thermocouple was cut on the outside surface and the thermocouple was inserted in this groove and brazed. There were 12 thermocouples at six axial distances installed at diametrically opposite locations. The system pressure was measured with the help of two Kellar make pressure transducers located on the pressuriser as well as at the heater outlet. The pressure drop across the bottom horizontal tube and the level in the pressuriser were measured with the help of two differential pressure transmitters. The power of each heater was measured with a Wattmeter. The secondary flow rate was measured with the help of a rotameter. All instruments were connected to a data logger with a user selectable scanning rate. For all the tests the selected scanning rate was 1 second.

The accuracy of the thermocouples were within ± 1.5 ^{0}C. The accuracy of the pressure and differential pressure measurements were respectively ± 0.03 MPa and ± 0.18 mm. The accuracy of the secondary flow as well as power measurement is ± 0.5 % of the reading. In addition, typical fluctuations of each instrument were also recorded during steady state with and without power. As seen from Table-1, there is hardly any difference in the fluctuations with and without power.

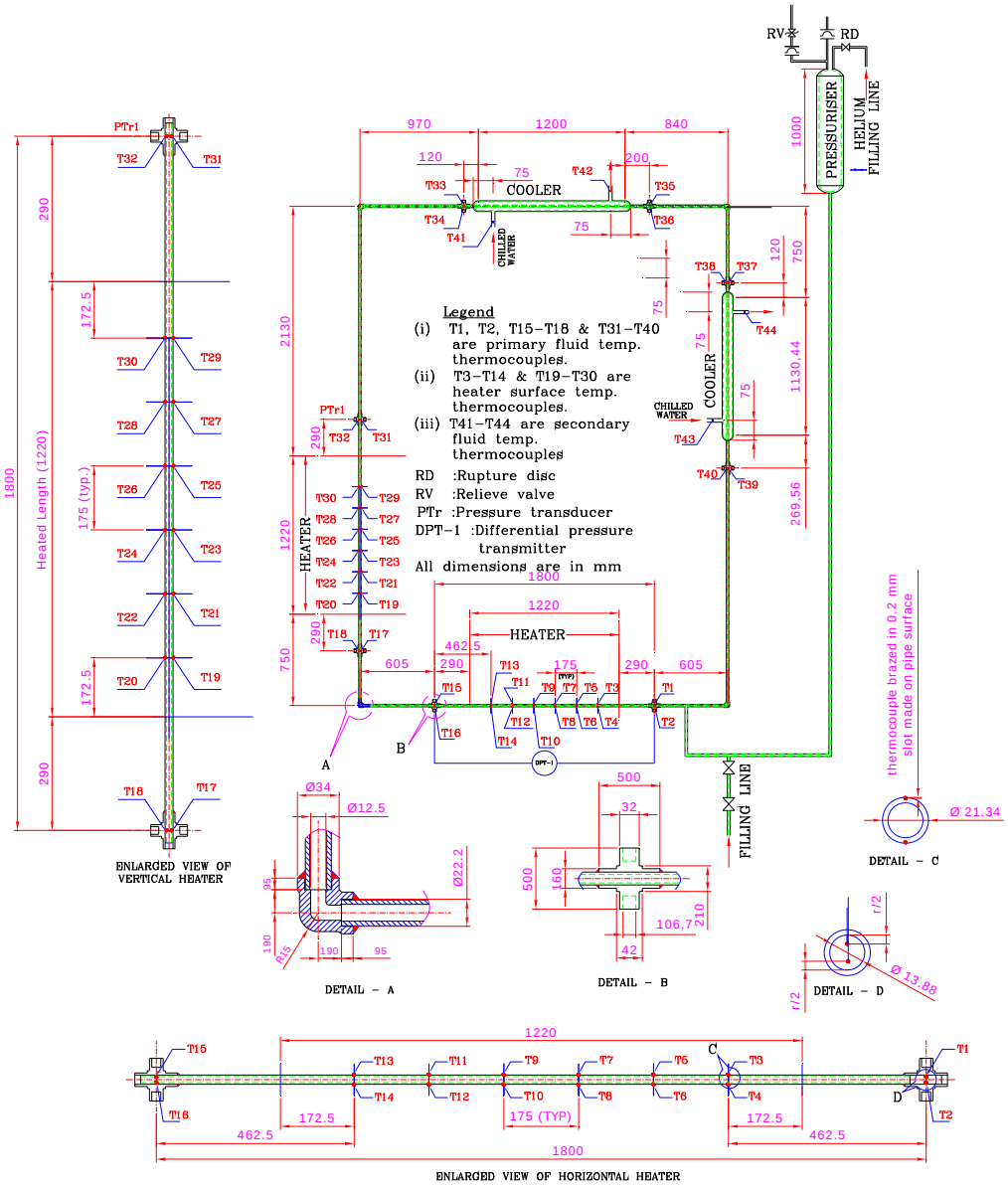

Figure 1 Supercritical pressure natural circulation loop (SPNCL)

2.2 Operation with Supercritical CO_2

Before operation with supercritical CO_2 the loop was flushed repeatedly with CO_2 at low pressure including all impulse, drain and vent lines. Subsequently the loop was filled with CO_2 up to 6 MPa pressure and the chilled water coolant was valved in. This caused condensation of CO_2 and hence a decrease in loop pressure. The pressure decrease was compensated by admitting additional CO_2 from

the cylinder and again allowed sufficient time for condensation. The process of filling and condensation was continued till there was no decrease in pressure. At this point the loop pressure was increased to the required value with the help of a helium gas cylinder. Once the required supercritical pressure was achieved, the helium cylinder was isolated. Sufficient time was allowed to reach a steady state. However, it was found difficult to attain completely stagnant conditions with uniform temperature throughout the loop as the higher ambient temperature allowed small amount of heat absorption through the insulation into the loop which was rejected at the cooler causing a small circulation rate. Once a steady state was achieved, the heater power was switched on and adjusted to the required value. Sufficient time was allowed to achieve the steady state. Once the steady state is achieved, power was increased and again sufficient time was provided to achieve the steady state. In case the system pressure increases beyond the set value by 0.1 MPa, a little helium was vented out to bring back the pressure to the original value. Similarly during power decrease if the pressure decreases below the set point by 0.1 MPa, then the loop was pressurized by admitting additional helium into the pressurizer. The experiments were repeated for different pressures and different chilled water flow rates. Subsequently the experiments were performed for different orientations of the heater and cooler.

Table-1: Fluctuations of measured parameters

Parameter	Fluctuation without power	Fluctuation under steady state natural circulation at 1400 W
Heater inlet temperature (^oC)	± 0.28	± 0.44
Heater outlet temperature (^oC)	± 0.44	± 0.43
Pressure (MPa)	± 0.028	± 0.028
Pressure drop (mm WC)	± 0.21	± 0.21
Secondary inlet temperature (^oC)	± 0.1	± 0.07
Secondary outlet temperature (^oC)	± 0.35	± 0.47

3. Steady State Natural Circulation Data for SPNCL

The SPNCL of BARC is actually a closed loop where heater inlet temperature is not controlled and only chilled water mass flow rate and inlet temperature on secondary side of cooler is maintained constant. Steady state data on natural circulation flow rate and heat transfer were generated with supercritical CO_2 for various orientations of the source and sink. The data ranges for each orientation is also given in table-2. The range of parameters of all the steady state data is

Orientations studied : HHHC, HHVC, VHHC and VHVC
Pressure : 8-9.2 MPa
Power : 0.1-2.4 kW
Cold leg temperature : 17.5-57.7 ^oC
Hot leg temperature : 19.3-95.9 ^oC
Coolant flow rate : 29.6-56 lpm
Coolant inlet temperature : 8.2-11.4 ^oC
Coolant outlet temperature : 9.0-12.5 ^oC

Table-2: Range of parameters for steady state tests with supercritical CO_2

Orientation	Power (kW)	Loop conditions			Secondary coolant conditions		
		Pressure (MPa)	Temperature (^oC)		Flow rate (lpm)	Temperature (^oC)	
			Cold leg	Hot leg		Inlet	Outlet
HHHC	0.19-2.4	8.5-9.2	17.7-57.7	20.5-95.9	29.6-37	8.7-10.2	9.5-11.7
HHVC	0.3-2.2	8.5-8.8	20.2-49.3	24.2-93.1	33.5-34.8	8.2-9.3	9-10.4
VHHC	0.14-2.4	9-9.26	17.5-49.5	19.6-73.9	31.6-38	8.5-11.4	9.7-12.5
VHVC	0.1-2.0	8.1-9.1	17.5-41.3	19.3-66.8	36.2-56	8.6-9.5	8.8-9.7

3.1 Steady State Natural circulation Flow Rate with Supercritical CO_2

Steady state data for the different heater-cooler orientations (i.e. HHHC, HHVC, VHHC & VHVC) generated in the loop were compared with the predictions of the in-house developed computer code NOLSTA [16] and the results are presented in figures 2a & 2b. The steady state mass flow rate for experimental conditions has been obtained as

$$W_{ss} = \text{Heater Power}/ (i_{out} - i_{in}) \quad (1)$$

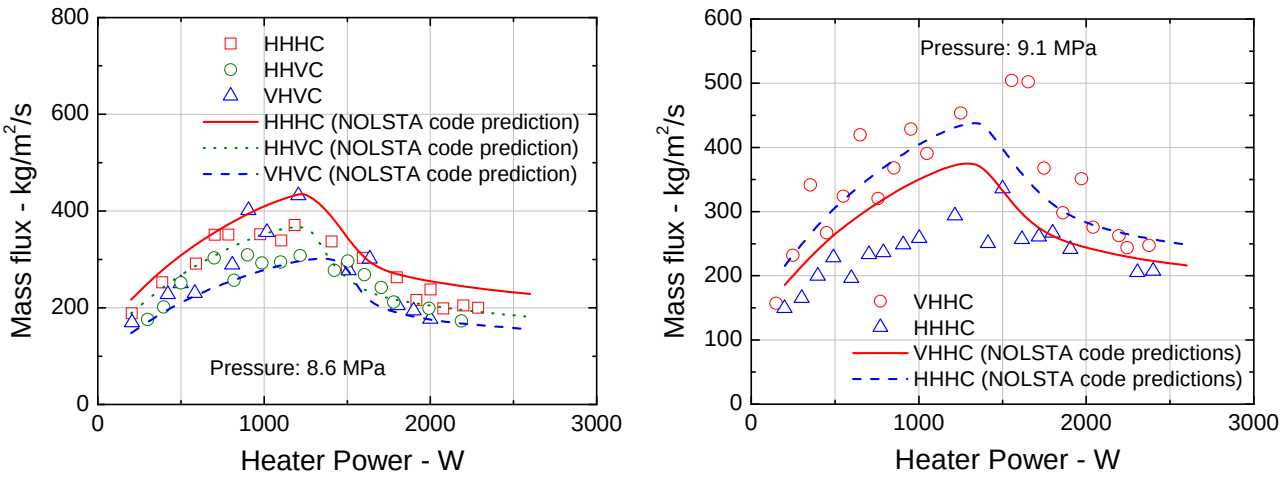

(2a) Steady state flow rate at 8.6 MPa

(2b) Steady state flow rate at 9.1 MPa

Figure 2 Measured and predicted steady state flow rate for various orientations

Enthalpy at heater outlet (i_{out}) can be calculated from heater outlet temperature and operating pressure measured experimentally and enthalpy at heater inlet (i_{in}) can be calculated from heater inlet temperature and operating pressure measured experimentally. The elbow loss coefficient has been taken to be 0.55 each (total 4 elbows) for predictions. Figure 2a shows the data for three different orientations for which data were available at 8.6 MPa. For the VHHC orientation data were available only for 9.1 MPa. The data for VHHC and HHHC orientations are compared with NOLSTA predictions in figure 2b. The data are found to be in close agreement with the code predictions. Higher mass flow rates are estimated experimentally for vertical heater orientation (i.e. VHVC & VHHC) as compared to NOLSTA code predictions. The maximum error associated with mass flow measurement is ± 30% for the loop operation near the pseudo-critical region, since the bulk fluid temperature

difference across the heater section is much less near the pseudo-critical region due to higher value of specific heat, whereas the error is much less away from the pseudo-critical region. The flow rates measured could not be verified by any other method i.e. heat balance of cooler, since the secondary side flow is quite high and does not show an appreciable change in temperature.

3.2 Effect of pressure

The data on the effect of pressure on the steady state flow rate are presented in figure 3 along with the predictions by the NOLSTA code. The mass flow rate reduces with increase in pressure which can be attributed to reduction in volumetric expansion coefficient with rise of pressure for supercritical fluids.

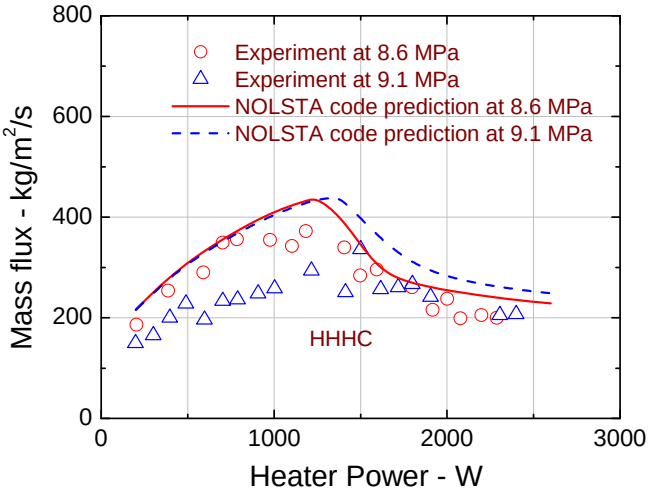

Figure 3 Effect of pressure on the steady state flow rate for the HHHC orientation

4. Experimental heat transfer coefficient for carbon-dioxide and comparison with various correlations

4.1 Determination of Heater heat transfer coefficient experimentally

The heat transfer coefficient in the heater is estimated from the measured outside surface temperature (T_{wo} *i.e. T3-T14*) of heater pipe at six equidistant locations along the length of each heater as shown in figure 4. At each location temperature is measured at two diametrically opposite positions (i.e. T3 & T4). Then, the steady state inside wall surface temperature of heater (T_{wi}) is estimated by a conduction analysis.

$$T_{wi} = T_{wo} - \frac{Q_{in} \ln\left(\frac{r_o}{r_i}\right)}{2\pi L k} \qquad (2)$$

Inlet and outlet fluid temperatures (T_{in} and T_{out} respectively) of heater are measured by using two thermocouples (T1 & T2 and T15 & T16 respectively) as shown in figure 4. The bulk fluid enthalpy at the corresponding location were obtained by the linear interpolation of enthalpies at inlet and outlet thermocouple readings as

$$i_b = i_{in} + \frac{x(i_{out} - i_{in})_h}{L} \quad (3)$$

From the local bulk enthalpy local fluid bulk temperature can be calculated. From local bulk temperature, inside heater wall temperature and heat input, the local heat transfer coefficient (h) can be estimated as given below:-

$$h = \frac{Q_{in}}{A(T_{wi} - T_b)} \quad (4)$$

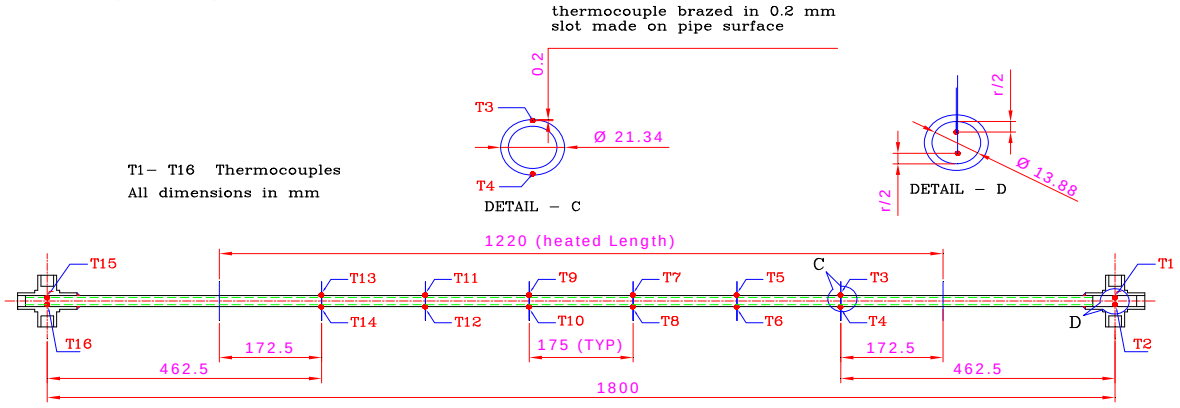

Figure 4 Instrumentation for measuring heat transfer coefficient in heater test

Uniform heat flux is assumed through out the heated length and A is the inside surface area of the tube. It may be noted that at a single power of operation in SPNCL, a complete temperature range of bulk fluid (i.e. sub-critical to supercritical) is not covered from heater inlet to heater outlet. Hence, the local heat transfer coefficient along horizontal heater length (HHHC orientation) has been determined for different operating powers corresponding to sub-critical, pseudo-critical and supercritical range of operation as shown in figures 5a, 5b& 5c respectively. For the horizontal heater, there are six thermocouples on the top and six at the bottom of the heater surface, hence two heat transfer coefficients are determined. At the entrance region the top heat transfer coefficient is higher but as the flow gets thermally developed the bottom heat transfer coefficient becomes larger. Buoyancy forces may enhance the heat transfer at tube bottom and reduce the same at the top of the tube. This is in agreement with experiments conducted for horizontal flow of carbon-dioxide at supercritical and sub-critical pressures [17]. They also found non-uniform cross-section temperature profile for horizontal flow and confirmed the effect of buoyancy forces by comparison with buoyancy free data. However, for vertical heater the wall temperatures don't vary much along the circumference at a fixed axial location, hence single heat transfer coefficient value is plotted along the length for vertical heater (VHVC orientation) as shown in figures 6a, 6b & 6c.

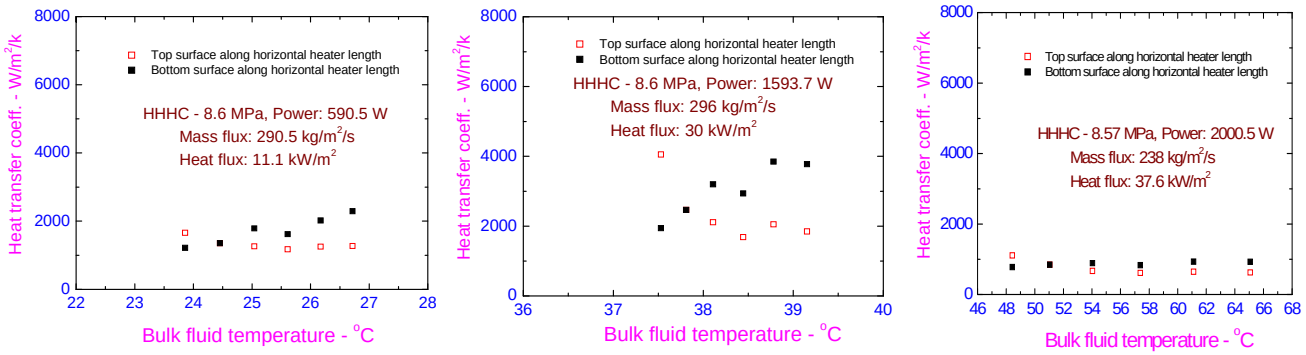

(5a) (5b) (5c)

Figure 5 Variation of heat transfer coefficient along horizontal heater length during sub-critical, pseudo-critical and supercritical temperature range of the bulk fluid

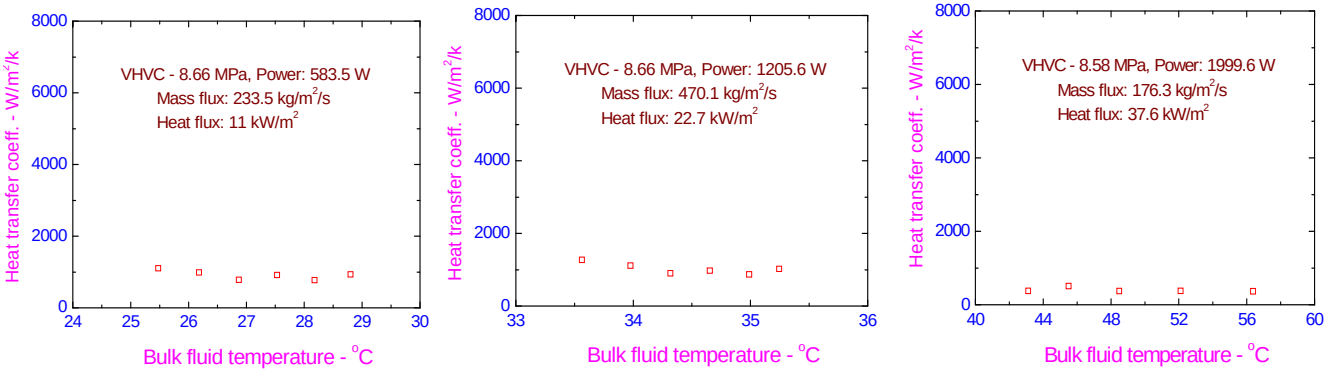

(6a) (6b) (6c)

Figure 6 Variation of heat transfer coefficient along vertical heater length during sub-critical, pseudo-critical and supercritical temperature range of the bulk fluid

The heat transfer coefficient is not varying significantly with the bulk carbon-dioxide temperature along the length of heater for the sub-critical, pseudo-critical and supercritical range of operation for horizontal or vertical heater. More over, no deterioration in heat transfer has been observed current range of operation of SPNCL. Hence, it is worth while to plot average heat transfer coefficient versus average bulk fluid temperature across heater section corresponding to various operating powers. Since the most correlations available in literature do not account for top and bottom heat transfer for horizontal flow, the average of top and bottom heat transfer has been taken in the results presented hereafter. The effect of pressure on heat transfer with carbon-dioxide at supercritical pressures is shown in figure 7. The peak of heat transfer coefficient reduces and shifts to higher bulk fluid temperature (just near pseudo-critical temperature) with increase of pressure. This may be because of reduction in peak specific heat and increase of pseudo-critical temperature with increase in pressure. The maximum and minimum heat transfer coefficient is observed for HHHC and VHVC orientation respectively as shown in figures 8a & 8b. This may be because of maximum natural circulation mass flow rate expected for HHHC orientation and minimum for VHVC orientation, as predicted by NOLSTA code in figures 2a & 2b, whereas experimental procedure to calculate the mass flow rate by energy balance over estimates the same for VHVC & VHHC orientations (see figures 2a & 2b). The maximum error associated with measurement of heat transfer coefficient is ± 15%.

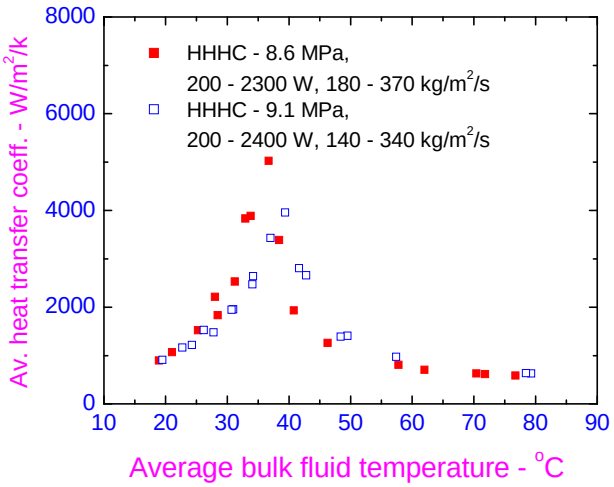

Figure 7 Effect of pressure on heat transfer coefficient

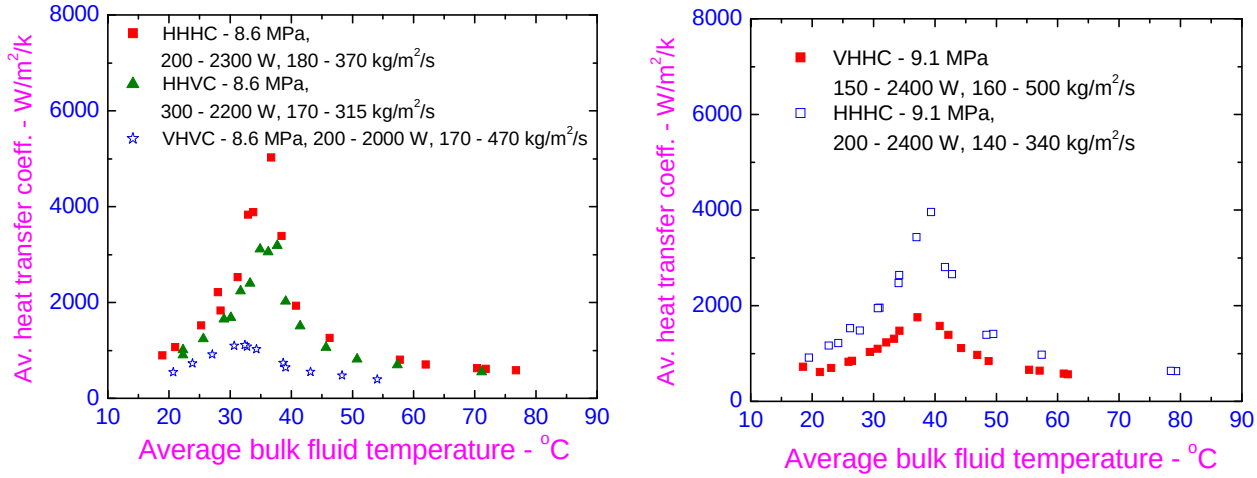

(8a) (8b)

FIG. 8 Effect of orientation on heat transfer coefficient

4.2 Comparison of heat transfer data with various empirical correlations

Subsequently the experimentally determined heat transfer coefficients for horizontal heater were compared with predictions of various correlations available in literature as shown in figures 9a, 9b & 9c. Most of the correlations i.e. Mc/Adams [18], Jackson [15], Bishop [20] and Shitsman [22] are showing good match with experimental heat transfer data for horizontal heater. This may be because of lower heat flux encountered during experimentation (max: 47 kW/m^2). A comparison for vertical heater orientation is shown in figures 10a, 10b & 10c. A large mismatch is found between experimental and predicted heat transfer coefficients for vertical heater. This may be attributed to higher flow rates estimated experimentally (using energy balance) for VHVC orientation (as it cannot be higher than HHHC orientation, see figure 2a) which goes as a direct input to correlations for calculating the Reynolds number, whereas heat transfer coefficient determined experimentally does not require mass flow rate as explained in section 4.1. However, Jackson Fewester [21], Shitsman [22] and Bishop [20] correlations are closer to experimental heat transfer results.

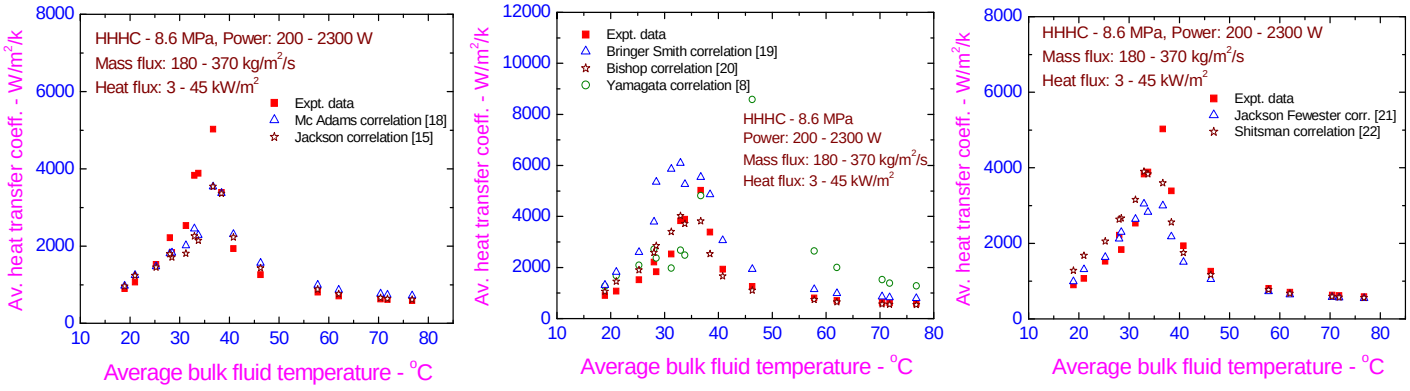

(9a) (9b) (9c)

Figure 9 Comparison of experimental heat transfer coefficient for horizontal heater with various correlations.

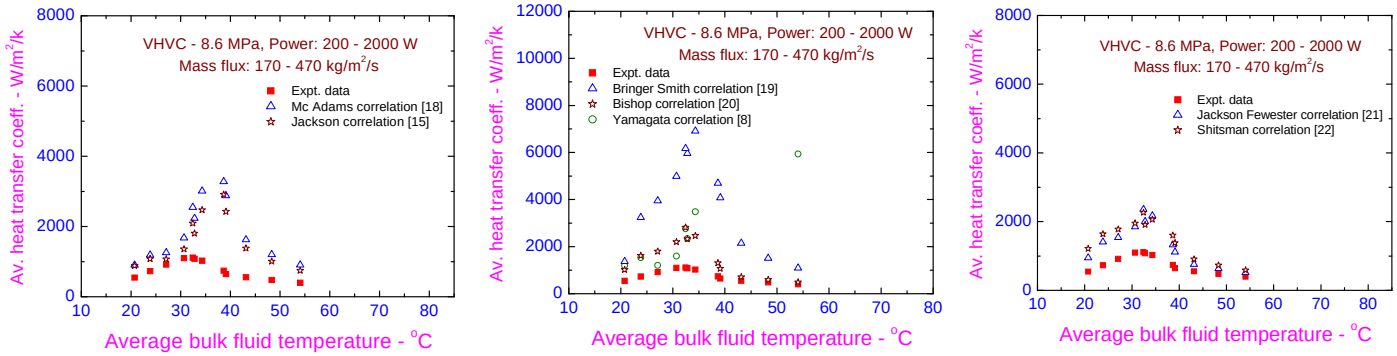

(10a) (10b) (10c)

Figure 10 Comparison of experimental heat transfer coefficient for vertical heater with various correlations.

5. Modification of the Facility for Operation with Supercritical Water

The existing ½" diameter supercritical natural circulation loop (SPNCL) was modified for operation with supercritical water which involved installation of new test sections, power supply and pressurizer. Two inconel heater test-sections (each for horizontal/ vertical heater) were fabricated. Thermocouples were brazed on the surface of each heater test section, at thirteen different axial locations. At each location, four thermocouples were provided at 90° angular distance (each at top, bottom, side-ways) as shown in figure 11.

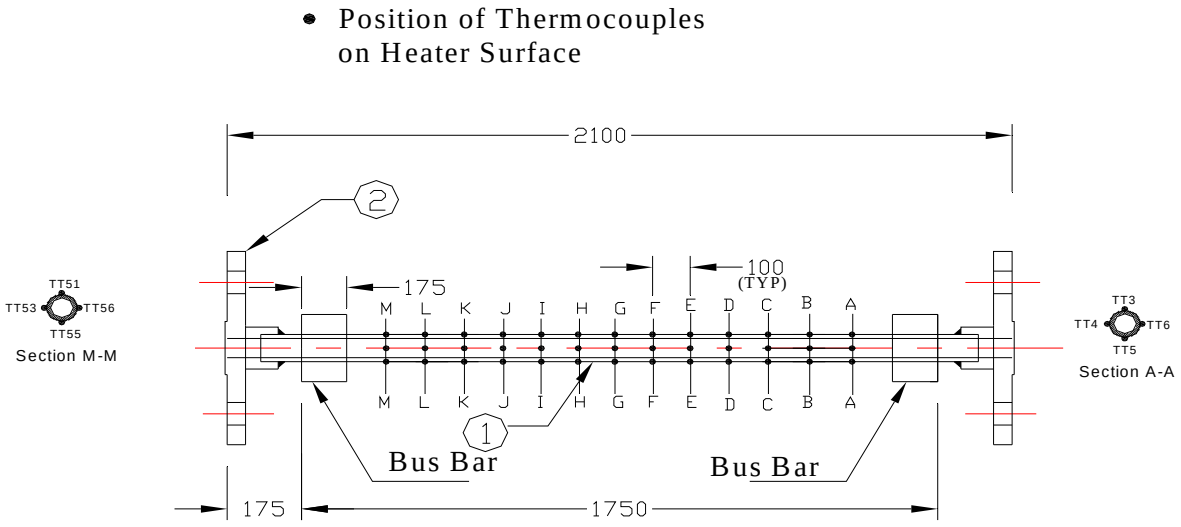

Figure 11 New horizontal/ vertical heater test section.

A 200 kW power supply (25 V & 8000 A) was installed and connected to the horizontal and vertical heater test sections by flexible couplings. The final dimensions of the augmented SPNCL are given in figure 12. The cooler is same, with air flowing in the secondary annular pipe. For this a large capacity air blower (i.e. 1600 cfm and 20 m WC head), has been installed and lines were laid connecting cooler to the blower. An anubar was installed in the 6" line for the air flow measurement.

6. Preliminary Steady State flow rate and heat transfer results with supercritical water

The experimental steady state mass flow rate, heater inlet and outlet temperatures versus power for constant secondary side air flow rate are shown in figure 13a & 13b respectively. The predictions by NOLSTA code are in close agreement with experimental data. The heater power however tripped at 8 kW, hence results are not available at this power. The heat transfer coefficient corresponding to above data were determined and compared with various heat transfer correlations available in literature for supercritical fluids as shown in figure 14a, 14b & 14c. Even though the mass flow rate is reducing after 6.5 kW of power (see figure 13a), the heat transfer coefficient has still increased by a factor of two approximately (the corresponding point for 6.5 kW power in figure 14a, b & c is at average bulk fluid temperature of 350 ^{o}C). Again the peak heat transfer coefficient is observed near the pseudo-critical temperature (corresponding power 7.5 kW in figure 13a and pressure 24 MPa). The heat transfer coefficient at bulk fluid temperatures higher than pseudo-critical temperatures could not be generated due to heater power trip. All correlations are giving good match for the sub-critical water heat transfer, whereas Mc/Adams [18], Jackson [15], Bringer Smith [19] and Shitsman [22] correlations are predicting well for pseudo-critical region.

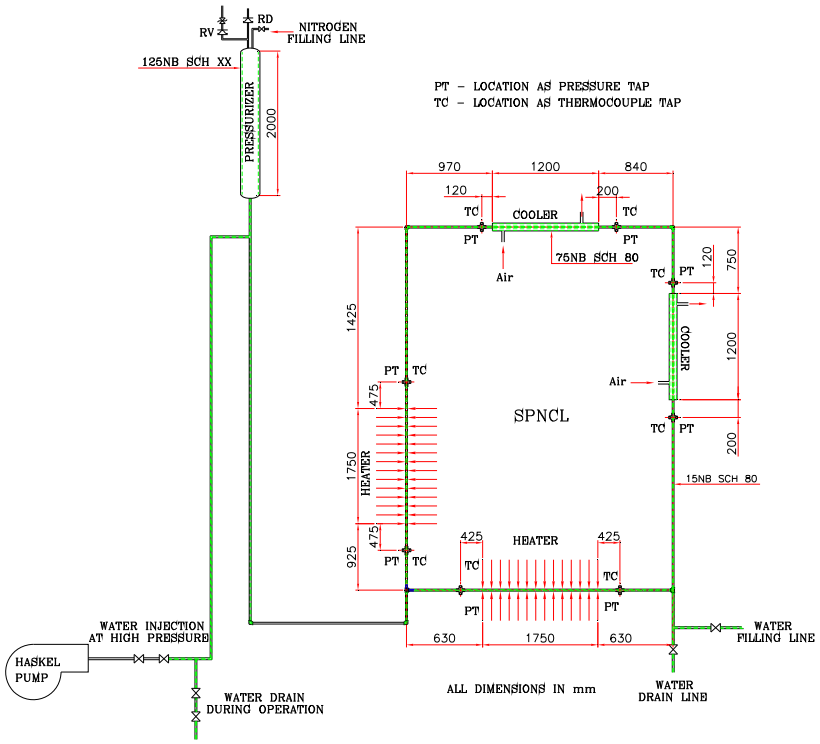

Figure 12 Schematic of Augmented SPNCL

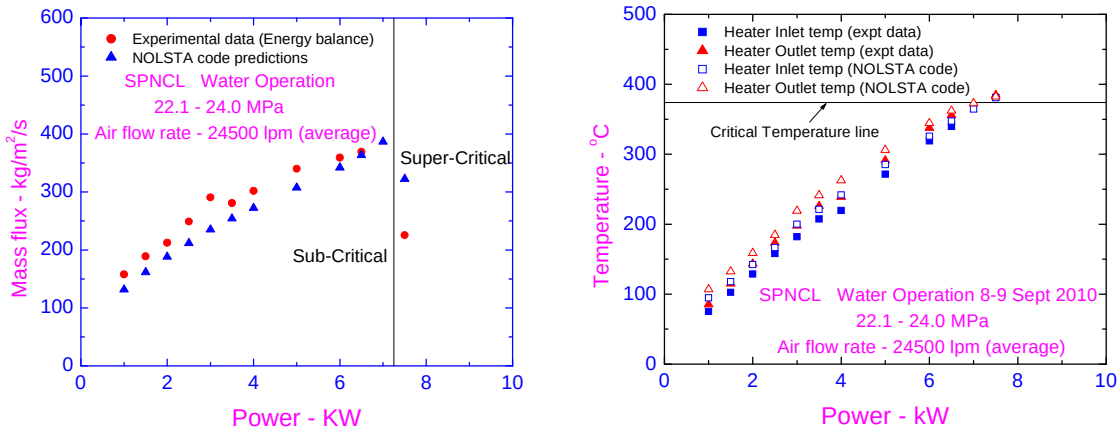

(13a) (13b)

Figure 13 Steady state characteristic of Augmented SPNCL (HHHC orientation)

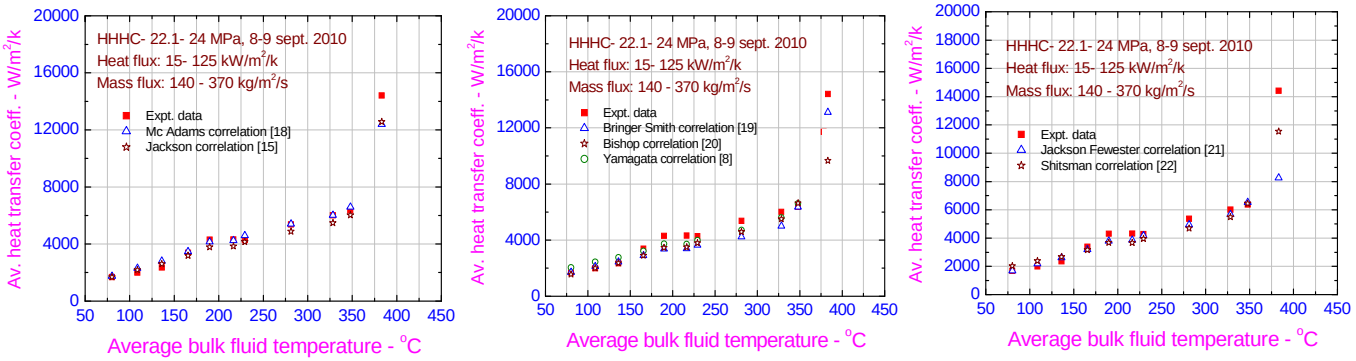

(14a) (14b) (14c)

Figure 14 Comparison of experimental heat transfer coefficient with various

7. Conclusions

Natural circulation experiments were conducted in SPNCL with carbon-dioxide and water at supercritical pressures. The data was analyzed for heat transfer under natural circulation conditions with both the fluids. During natural circulation as the heat flux is increased the mass flux first increases and then decreases, but no deterioration was observed for the range of experimentation with both fluids. This may be due to lower values of heat flux (maximum: 47 kW/m^2 for carbon-dioxide and 125 kW/m^2 for water) used during the experiments. Peak values of heat transfer coefficient are observed very near the pseudo-critical temperature for both the fluids. With increase of pressure the peak of heat transfer coefficient reduces and shifts to higher bulk fluid temperature as observed for carbon-dioxide. For horizontal heater the bottom heat transfer coefficient is found to be higher than the top because buoyancy forces assist heat transfer at the bottom surface. For horizontal heater operation with carbon-dioxide or water, all correlations are giving good match for the heat transfer at sub-critical and supercritical region (i.e. far away from pseudo-critical region), whereas Mc/Adams [18], Jackson [15] and Shitsman [22] correlations are predicting well in the pseudo-critical region. For vertical heater operated with only carbon-dioxide, lot of deviation has been found between the experimental heat transfer and that predicted by the correlations. This may be attributed to overestimation of experimental flow rates determined by energy balance for VHVC and VHHC orientation. However, Jackson Fewester [21], Shitsman [22] and Bishop [20] correlations predict closer to experimental heat transfer results for vertical heater configuration.

NOMENCLATURE

A	Heat transfer area (m^2)
H	Heat transfer coefficient (W/m^2/k)
I	Enthalpy (J/kg)
K	Thermal conductivity (W/m/k)
L	Length of a heater section (m)
R	Radius (m)
W	Mass flow rate (kg/s)
x	Axial distance (m)

Subscripts

B	bulk
H	heater
I	inside
In	inlet
O	outside
out	outlet
Ss	steady state
W	wall

REFERENCES

1) Oka, Y. (2000), "Review of high temperature water and steam cooled reactor concepts", SCR-2000, Nov.6-8, 2000, Tokyo, Paper 104.
2) Oka, Y. and Koshizuka, S. (1993), "Concept and design of a supercritical-pressure, direct-cycle light water cooled reactor", Nuclear Technology 103, 295–302.
3) Oka, Y. and Koshizuka, S. (2000), "Design concept of once-through cycle supercritical light water cooled reactors", SCR-2000, Nov.6-8, 2000, Tokyo, Paper 101.
4) Heusener, G., Muller, U., Schulenberg, T., Squarer, D. (2000), "A European development program for a high performance light water reactor (HPLWR)", SCR-2000, Nov.6-8, 2000, Tokyo, Paper 102.
5) Zhao, J., Saha, P. and Kazimi, M.S., (2005), "Stability of supercritical water-cooled reactor during steady-state and sliding pressure start-up", NURETH-11, October 2-6, Avignon, France.
6) Silin V.A., Voznesensky, V.A. and Afrov, A.M., (1993), "The light water integral reactor with natural circulation of the coolant at supercritical pressure B:500 SKDI", Nuclear Engineering and Design 144, 327-336.
7) Bushby, S.J., Dimmick, G.R., Duffey, R.B., Spinks, N.J., Burrill, K.A. and Chan, P.S.W., "Conceptual designs for advanced, high-temperature CANDU reactors", SCR-2000, Nov.6-8, 2000, Tokyo, Paper 103.
8) Yamagata, K., Nishikawa, K., Hasegawa, S., et al., 1972, "Forced convective heat transfer to supercritical water flowing in tubes", Int. J. Heat Mass Transfer 15 (12), 2575–2593.
9) Swenson, H.S., Carver, J.R., Karakala, C.R., 1965, "Heat transfer to supercritical water in smooth-bore tubes", J. Heat Transfer, Trans. ASME, Ser. C 87 (4), 477–484.
10) Jackson, J.D., Lutterodt, K.E., Weinberg, R., 2003, "Experimental studies of buoyancy-influenced convective heat transfer in heated vertical tubes at pressures just above and just below the thermodynamic critical value", Proceedings of the GENES4/ANP, 15–19 September, Kyoto, Japan. Paper 1177.
11) Fewster, J., Jackson, J.D., 2004, "Experiments on supercritical pressure convective heat transfer having relevance to SCWR",Proceedings of the International Congress on Advances in Nuclear Power Plants (ICAPP'04), 13–17 June, Pittsburgh, USA. Paper 4342.
12) I. L. Pioro and R.B. Duffey, 2005, "Experimental heat transfer to supercritical water flowing inside channels (Survey)", Nucl. Eng. Design, 235 (22), 2407.
13) R.B. Duffey and I.L. Pioro, 2005, "Experimental heat transfer of supercritical carbon dioxide flowing inside channels (Survey)", Nucl. Eng. Design, 235 (8), 913.

14) Pioro, I.L., Khartabil, H.F., Duffey, R.B., 2004, "Heat transfer to supercritical fluids flowing in channels–empirical correlations (survey)". Nuclear Eng. Design 230 (1–3), 69-91.
15) Jackson, J.D., 2002, "Consideration of the heat transfer properties of supercritical pressure water in connection with the cooling of advanced nuclear reactors", Proceedings of the 13th Pacific Basin Nuclear Conference, 21–25 October, Shenzhen City, China..
16) Sharma M., P.K. Vijayan, D.S. Pilkhwal, D. Saha and R.K. Sinha, "Linear and non-linear stability analysis of a supercritical natural circulation loop", ASME Journal of Engineering for Gas Turbines and Power, October 2010, Vol. 132 / 102904-1.
17) Adebiyi, G.A., Hall,W.B., 1976 "Experimental investigation of heat transfer to supercritical pressure carbon dioxide in a horizontal tube", Int. J. Heat Mass Transfer 19 (7), 715–720.
18) McAdams, W.H., 1942. Heat Transmission, 2nd edition, McGraw-Hill, New York, NY, USA.
19) Bringer, R.P., Smith, J.M., 1957,"Heat transfer in the critical region", AIChE J. 3 (1), 49–55.
20) Bishop, A.A., Sandberg, R.O., Tong, L.S., 1964,"Forced convection heat transfer to water at near-critical temperatures and supercritical pressures", Report WCAP-2056, Part IV, November, Westinghouse Electric Corp., Pittsburgh, USA.
21) Jackson, J.D., Fewster, J., 1975"Forced convection data for supercritical pressure fluids", HTFS 21540.
22) Shitsman, M.W., 1974,"Heat transfer to supercritical helium, carbon-dioxide, and water: analysis of thermodynamic and transport properties and experimental data", Cryogenics 14 (2), 77–83.